Fingered core structure of nematic boojums

Samo Kralj
Faculty of Natural Sciences and Mathematics, University of Maribor, 2000 Maribor, Slovenia
and Jožef Stefan Institute, P.O. Box 3000, 1001 Ljubljana, Slovenia

Riccardo Rosso and Epifanio G. Virga
Dipartimento di Matematica and CNISM, Università di Pavia, via Ferrata 1, I-27100 Pavia, Italy
(Received 27 February 2008; revised manuscript received 4 July 2008; published 2 September 2008)

Using the Landau–de Gennes phenomenological approach, we study the fine biaxial core structure of a boojum residing on the surface of a nematic liquid crystal phase. The core is formed by a negatively uniaxial finger, surrounded by a shell with maximal biaxiality. The characteristic finger's length and the shell's width are comparable to the biaxial correlation length. The finger tip is melted for topological reasons. Upon decreasing the surface anchoring strength below a critical value, the finger gradually leaves the bulk and it is expelled through the surface.

DOI: 10.1103/PhysRevE.78.031701 PACS number(s): 61.30.Jf, 61.30.Dk, 61.30.Hn

Topological defects have attracted scientists' interest for years. They are ubiquitous, being retraced in branches of physics as diverse as cosmology and condensed matter physics. The first theory of topological defects was indeed proposed by cosmologists [1] to explain the coarsening dynamics of the defect tangle in the early universe. Now, it is also believed that defects significantly influence the structure of universe [2]. More recently, with the proposal of Nelson [3,4] to do chemistry by using colloidal particles instead of atoms, surface defects on thin nematic liquid crystal (LC) shells coating nanoparticles have been shown to play a central role in determining the colloidal's valence, and with it the pattern they are likely to produce by mutual binding [5]. Defects are classified into different classes according to their topological charge by the homotopy group theory [6]. This charge is a conserved quantity and controls the transformations of defects (merging, annihilation, decaying). In general, for their remarkable optical properties, nematic LCs are particularly appropriate media to study many classes of defects. Here we shall only consider point defects. A point defect can reside either in the bulk or on the boundary of the region $\mathcal{B}$ occupied by a LC; the former is usually called a "hedgehog," while the latter is called a "boojum" [7,8]. Both types of defects have an inner biaxial structure of their own, the core. The equilibrium core of a hedgehog is rather well understood, but it is still unclear whether boojums have a distinctive core structure, different from that of hedgehogs. One might intuitively expect the boojum's core to be obtained by severing the hedgehog's core into two halves, retaining only one, as sketched in Fig. 1(a). In this paper, we show that for strong enough surface anchorings a boojum spontaneously protrudes into the bulk a robust, negatively uniaxial finger bearing an isotropic tip, as illustrated in Fig. 1(b).

The nematic ordering is described in terms of the second-rank, symmetric, traceless tensor [9]

$$\mathbf{Q} = \sum_{i=1}^{3} \lambda_i \mathbf{e}_i \otimes \mathbf{e}_i, \tag{1}$$

where $\lambda_i \in [-\frac{1}{2}, 1]$ and $\mathbf{e}_i$ are the ith eigenvalue and the ith eigenvector of $\mathbf{Q}$, respectively. Weakly distorted textures exhibit a uniaxial ordering represented by

$$\mathbf{Q} = S\left(\mathbf{n} \otimes \mathbf{n} - \frac{1}{3}\mathbf{I}\right), \tag{2}$$

where $\mathbf{I}$ is the identity. The nematic director $\mathbf{n}$ identifies the local uniaxial ordering direction and the uniaxial order parameter S measures fluctuations about this direction. The degree of biaxiality of $\mathbf{Q}$ is measured by the positive parameter $\beta^2 := 1 - \frac{6(\mathrm{tr}\mathbf{Q}^3)^2}{(\mathrm{tr}\mathbf{Q}^2)^3} \leqslant 1$. The value $\beta^2 = 0$ represents a uniaxial ordering and the value $\beta^2 = 1$ represents an ordering with the maximum degree of biaxiality.

We express the free energy of the system as the sum $F = \int_{\mathcal{B}} (f_b + f_e) dv + \int_{\partial\mathcal{B}} f_s da$ of volume and surface integrals [10–12]:

$$f_b = \frac{a(T - T_*)}{2}\mathrm{tr}\mathbf{Q}^2 - \frac{B}{3}\mathrm{tr}\mathbf{Q}^3 + \frac{C}{4}(\mathrm{tr}\mathbf{Q}^2)^2, \tag{3}$$

$$f_e = \frac{L}{2}|\nabla\mathbf{Q}|^2, \tag{4}$$

$$f_s = \frac{w}{2}\mathrm{tr}(\mathbf{Q} - \mathbf{Q}_s)^2. \tag{5}$$

Here T is the temperature, T_* is the supercooling temperature, a, B, and C are positive material constants, $L > 0$ is the elastic constant, $|\nabla\mathbf{Q}|^2$ is the square norm of the order tensor gradient (a third-rank tensor), w is the anchoring strength and $\mathbf{Q}_s$ is the order tensor preferred at the boundary $\partial\mathcal{B}$. The bulk term f_b enforces a homogeneous nematic alignment with $S = s_b := s_0(1 + \sqrt{1 - \theta})$ for $\theta \leqslant \frac{T_{IN} - T_*}{T_{**} - T_*} = \frac{8}{9}$, where $\theta := \frac{24aC}{B^2} = \frac{T - T_*}{T_{**} - T_*}$ is the reduced temperature, T_{**} is the superheating temperature, T_{IN} the bulk transition temperature, and $s_0 := \frac{B}{4C}$. We further introduce the surface extrapolation length $d_e := L/w$ and the biaxial correlation length $\xi_b := \sqrt{\frac{4LC}{B^2(\sqrt{1-\theta}+1)}}$. In conventional nematics $\xi_b \sim 20$ nm.

As a representative boojum, we study the one induced on the plate with planar, degenerate anchoring of a cylindrical hybrid cell with thickness h and width $2R$ (see Fig. 2). The

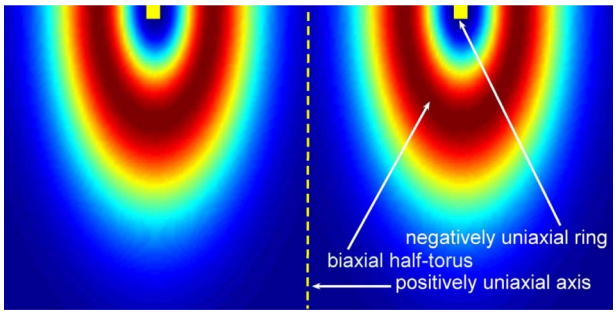

(a)

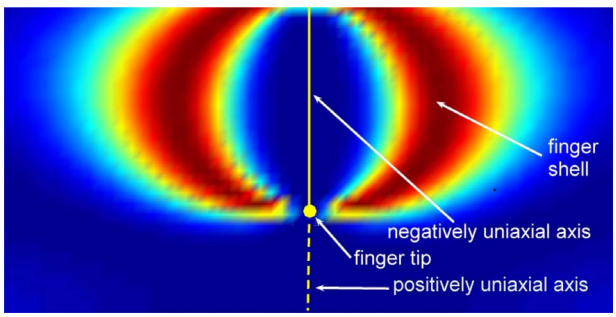

(b)

FIG. 1. (Color online) Cross section orthogonal to the surface hosting the defect (here on the top) of half a hedgehog (a) and a fingered boojum (b), both showing a contour plot of the degree of biaxiality β^2. Brighter contours correspond to larger values of β^2, darker contours correspond to smaller values of β^2. In (a) a biaxial half-torus with maximum biaxiality encircles a negatively uniaxial ring coming out of the section plane; two squares represent its traces. The symmetry axis is positively uniaxial. In (b) a biaxial shell joins the isotropic finger tip with the top surface. The negatively uniaxial finger is the thick solid line along the symmetry axis.

cell is described in a cylindrical coordinate system $\{r,\vartheta,z\}$, with axes pointing along the unit vectors $\{\mathbf{e}_r,\mathbf{e}_\vartheta,\mathbf{e}_z\}$. At the bottom plate ($z=0$) we impose the strong homeotropic anchoring. At the top plate ($z=h$) a point defect results from setting $\mathbf{Q}_s=s_b(\mathbf{e}_r\otimes\mathbf{e}_r-\frac{1}{3}\mathbf{I})$ in Eq. (5) with a finite anchoring strength w. We set free boundary conditions at the cell's lateral boundary. For computational purposes, we represent $\mathbf{Q}$ in terms of the parameters $\{q_0,q_\delta,q_m\}$ as

$$\mathbf{Q}=-2q_0\mathbf{e}_\vartheta\otimes\mathbf{e}_\vartheta+(q_0+q_\delta)\mathbf{e}_r\otimes\mathbf{e}_r+(q_0-q_\delta)\mathbf{e}_z\otimes\mathbf{e}_z+q_m(\mathbf{e}_r\otimes\mathbf{e}_z+\mathbf{e}_z\otimes\mathbf{e}_r). \tag{6}$$

The parameter q_m signals departures of the eigenframe of $\mathbf{Q}$ from $\{\mathbf{e}_r,\mathbf{e}_\vartheta,\mathbf{e}_z\}$, while either $q_\delta^2+q_m^2=0$ or $q_\delta^2+q_m^2=9q_0^2$ wherever $\mathbf{Q}$ is uniaxial. This parametrization only allows for rotations of the eigenframe of $\mathbf{Q}$ about $\mathbf{e}_\vartheta$. We restrict our attention to cylindrically symmetric solutions where the parameters q's depend only on the coordinates r and z. We scale all q's to s_0, and the spatial coordinates to h. The volume free-energy densities, scaled to $2Cs_0^4$, can be expressed as

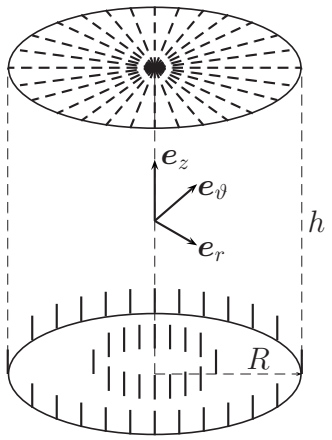

FIG. 2. Sketch of a cylindrical hybrid cell.

$$f_b=\frac{\theta}{3}(q_m^2+q_\delta^2+3q_0^2)-4q_0(q_m^2+q_\delta^2-q_0^2)+\frac{1}{2}(q_m^2+q_\delta^2+3q_0^2)^2, \tag{7}$$

$$f_e=\frac{2\xi_b^2(1+\sqrt{1-\theta})}{h^2}\left[3|\nabla q_0|^2+|\nabla q_\delta|^2+|\nabla q_m|^2+\frac{(3q_0+q_\delta)^2+q_m^2}{r^2}\right], \tag{8}$$

where ∇ is the dimensionless gradient and the q's now denote the scaled parameters. We minimize the total free energy by solving numerically the resulting Euler-Lagrange equations with the over-relaxation method [13]. We used different ansatzs as initial guesses, with both uniaxial and biaxial configurations; the relaxed solution proved to be extremely robust for all these choices.

For presentation purposes, we also introduce the following equivalent parametrization in Eq. (1), particularly fit to represent changes in the eigenvalues of $\mathbf{Q}$:

$$\mathbf{e}_1=\sin\varphi\mathbf{e}_r+\cos\varphi\mathbf{e}_z,\quad \mathbf{e}_2=\mathbf{e}_\vartheta, \tag{9}$$

$$\mathbf{e}_3=-\cos\varphi\mathbf{e}_r+\sin\varphi\mathbf{e}_z, \tag{10}$$

$$\lambda_1=\frac{2}{3}s\cos\psi,\quad \lambda_2=-\frac{2}{3}s\cos\left(\psi-\frac{\pi}{3}\right), \tag{11}$$

$$\lambda_3=-\frac{2}{3}s\cos\left(\psi+\frac{\pi}{3}\right). \tag{12}$$

It follows from Eqs. (11) and (12) that $s=\sqrt{\frac{3}{2}\mathrm{tr}\mathbf{Q}^2}$. Possible nematic states in a given eigenframe $\{\mathbf{e}_1,\mathbf{e}_2,\mathbf{e}_3\}$ are represented in the phase space $\{s,\psi\}$ shown in the inset to Fig. 5 (for details, see Ref. [11]). The parametrizations $\{q_0,q_\delta,q_m\}$ and $\{\varphi,\psi,s\}$ are related via the equations $q_0=\frac{s}{3}\cos(\psi-\frac{\pi}{3})$, $q_m=\frac{s}{3}\sin 2\varphi[\cos(\psi+\frac{\pi}{3})+\cos\psi]$, and $q_\delta=-\frac{s}{3}\cos 2\varphi[\cos(\psi+\frac{\pi}{3})+\cos\psi]$. Thus, for example, the points $\{\varphi,\psi\}$ and $\{\varphi+\frac{\pi}{2},\frac{2\pi}{3}-\psi\}$ in the phase space represent one and the same state.

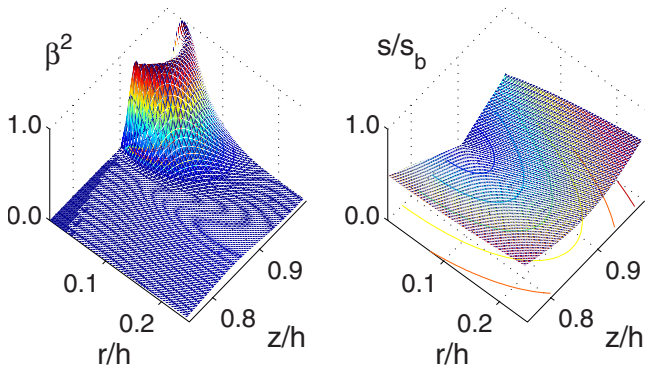

FIG. 3. (Color online) The functions β^2 and s/s_b on the (r,z) plane. The finger tip is located at $r=0$ and $z=h-\xi_f\approx 0.83h$. Here, as in Fig. 1(b), we set $h/\xi_b=10$, $R=h$, and $h/d_e=10$. For these parameters, a finger is well developed.

We now describe in this language the half-hedgehog depicted in Fig. 1(a). The hedgehog core structure is biaxial [11,12,14–16] and cylindrically symmetric. Its positively uniaxial symmetry axis ($S>0$) is surrounded by a negatively uniaxial ring ($S<0$), which is further enclosed within a torus [11] exhibiting maximal degree of biaxiality ($\beta^2=1$). To picture a boojum as half a hedgehog, we artificially enforce the radial field for $\mathbf{e}_1$ ($\varphi=\pi/2$) at the cell's top plate, while imposing no constraints on the eigenvalues of $\mathbf{Q}$. The symmetry axis then turns out to be positively uniaxial. On approaching it radially from a distance much larger than ξ_b at $z=h$ [top plate in Fig. 1(a)], the nematic state traces the path from $\psi=0$ (for which $\mathbf{n}=\mathbf{e}_1=\mathbf{e}_r$) toward $\psi=2\pi/3$ (for which $\mathbf{n}=\mathbf{e}_3=\mathbf{e}_z$). The corresponding β^2 profile exhibits two hills, on top of which $\beta^2=1$, separated by a negatively uniaxial ring, where $\beta^2=0$ [11].

However, our numerical solution for a real boojum yields a qualitatively different, but topologically consistent core [see Fig. 1(b)]. We consider a finite anchoring strength at the top plate and calculate the equilibrium boojum core structure as w is varied. The symmetry axis must be always uniaxial for f_e to be integrable at $r=0$: see the last term in Eq. (8). Uniaxial states oriented along $\mathbf{e}_z$ correspond to $3q_0=-q_\delta$; they are represented by Eq. (2) with $\mathbf{n}=\mathbf{e}_z$ and $S=6q_0$. In our explorations, h/d_e ranges from 5 to 100. We first consider a relatively strong anchoring condition ($h/d_e>10$). The top surface strongly favors uniaxial states (i.e., $\beta^2=0$), and the core structure is characterized by a "finger" protruding into the cell's interior along its symmetry axis (see Fig. 3). We refer to such a core structure as the "fingered" boojum [see also the contour plot of β^2 in Fig. 1(b)]. The representative cross-section profiles of $\varphi(r,z)$, $s(r,z)$, and $\beta^2(r,z)$ are shown in Fig. 4. The finger is negatively uniaxial ($S<0$) and it ends in a melted (isotropic) point ($S=0$) at the distance $\xi_f\sim\xi_b$ from the surface (Fig. 3); this is the finger tip, where the state becomes positively uniaxial ($S>0$). The finger is enclosed within a biaxial shell with $\beta^2=1$, which joins the finger tip with the surface [see Fig. 1(b)]. For a given finite value of w, the average order parameter s melts only at the finger tip. The length-scale over which s approaches zero compares with the uniaxial nematic correlation length, which in the deep nematic phase is shorter than ξ_b.

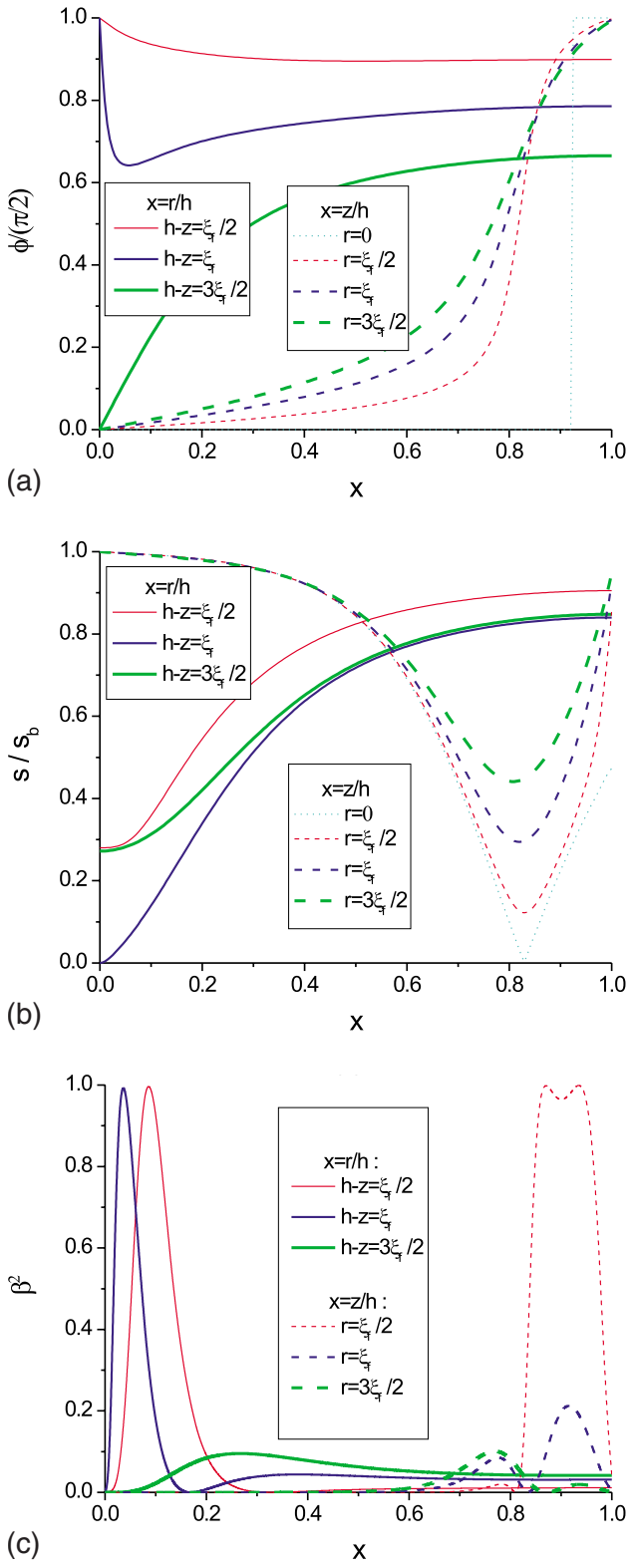

FIG. 4. (Color online) Representative cross sections of (a) $\varphi(r,z)$, (b) $s(r,z)$, and (c) $\beta^2(r,z)$ for a structure similar to that shown in Fig. 3. The variations along r and z are marked with solid and dashed lines, respectively. Both solid and dashed lines are associated with different sections through their thickness. The dotted lines in (a) and (b) correspond to the radial trajectory in Fig. 5. Here, $h/\xi_b=20$, $R=h$, and $h/d_e=100$.

The observed core structure is forced by topological reasons. This can be seen by mapping the boojum structure into the phase space $\{s,\psi\}$. To illustrate this, we take representative paths across the boojum core structure in the real space and track back the corresponding excursions in the phase space. To this purpose, we start from the axis of cylindrical symmetry, close to the finger's midpoint. We first move along the axis toward the bottom plate. The path in the $\{s,\psi\}$ plane is depicted in the inset to Fig. 5 by a radial trajectory. The corresponding variations in real space are shown by the dotted lines in Figs. 4(a) and 4(b). One sees that going from negatively to positively uniaxial states the melting point (corresponding to the origin of the $\{s,\psi\}$ plane) is unavoidable [see Fig. 4(b)]. We next move radially from the same starting point toward the lateral boundary of the cell, where the ordering is essentially uniaxial (see the other trajectory in the inset to Fig. 5 and the thinnest solid graphs in Figs. 4). One sees that in this case the shell with $\beta^2=1$, which possesses a positive value of s and surrounds the finger, must necessarily be crossed. Upon decreasing w, the finger tip gradually approaches the surface and the fingered boojum exits the cell through the upper plate at $h/d_e \approx 5$ (solid line in Fig. 5). Thus, for the chosen surface potential, a boojum does not transform itself into half a hedgehog. One can artificially induce such a transformation by decreasing the anchoring strength, but only if the anchoring for the eigenframe of $\mathbf{Q}$ remains much stronger than the anchoring for its eigenvalues. In conclusion, we studied the core of a representative boojum. Boojums are experimentally most commonly realized in essentially spherical nematic droplets with relatively strong tangential anchoring, although the setting assumed in our modelling was also experimentally implemented [17]. Our model also applies to droplets whenever their radius of curvature is large with respect to ξ_b; the cylindrical symmetry assumed in our computations merely makes them easier. We have shown that for most common anchoring conditions a fingered boojum is formed, which is characterized by a negatively uniaxial finger extending from the boundary toward the interior and ending in a melted point. To ease presentation, the core was shown in a cylindrical cell of thickness $h=20\xi_b$ and radius $R=h$. Thus, the far director field influences the core structure quantitatively, but not qualitatively [11]. For example, upon increasing h, the characteristic finger length ξ_f at first gradually increases and then saturates at $\xi_f \approx 4\xi_b$ (dashed line in Fig. 5).

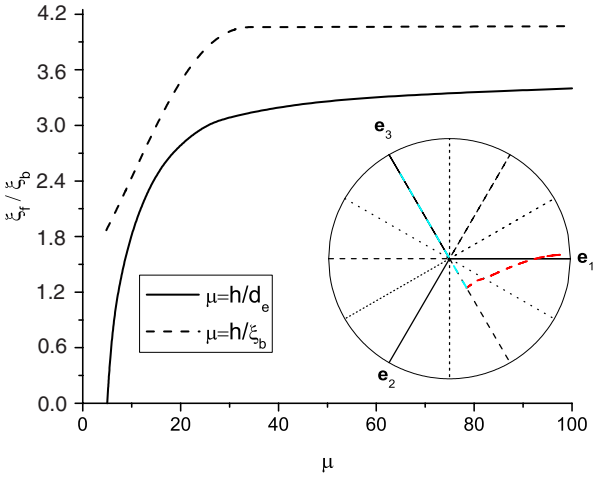

FIG. 5. (Color online) The finger length ξ_f as a function of the cell thickness (dashed line, strong anchoring) and as a function of the anchoring strength (solid line, $h/\xi_b=20$). For both curves, $R=h$. Inset: nematic states in the phase space $\{s,\psi\}$. Solid radial lines: positively uniaxial states ($S>0$) with $\mathbf{n}=\mathbf{e}_i$ ($i=1$, $\psi=0$; $i=2$, $\psi=-\frac{2\pi}{3}$; $i=3$, $\psi=\frac{2\pi}{3}$). Dashed radial lines: negatively uniaxial states ($S<0$) with $\mathbf{n}=\mathbf{e}_i$ ($i=1$, $\psi=\pi$; $i=2$, $\psi=\frac{\pi}{3}$; $i=3$, $\psi=-\frac{\pi}{3}$). Dotted radial lines: states with maximal degree of biaxiality ($\beta^2=1$). The circle corresponds to $s=s_b$. Two trajectories emanating from one and the same point, one of which is superimposed to the radial uniaxial lines with $\mathbf{n}=\mathbf{e}_3$, describe order variations corresponding to graphs shown in Figs. 4.

[1] T. W. B. Kibble, J. Phys. A **9**, 1387 (1976).
[2] U. Nucamendi, M. Salgado, and D. Sudarsky, Phys. Rev. Lett. **84**, 3037 (2000).
[3] D. R. Nelson, Nano Lett. **2**, 1125 (2002).
[4] V. Vitelli and D. R. Nelson, Phys. Rev. E **74**, 021711 (2006).
[5] G. Skačej and C. Zannoni, Phys. Rev. Lett. **100**, 197802 (2008).
[6] M. Kleman and O. D. Lavrentovich, *Soft Matter Physics* (Springer, New York, 2003).
[7] G. E. Volovik and O. D. Lavrentovich, Zh. Eksp. Teor. Fiz. **85**, 1997 (1983) [Sov. Phys. JETP **58**, 1159 (1983)].
[8] H. R. Trebin and R. Kutka, J. Phys. A **28**, 2005 (1995).
[9] E. G. Virga, *Variational Theories for Liquid Crystals* (Chapman and Hall, London, 1994).
[10] P. G. de Gennes and J. Prost, *The Physics of Liquid Crystals* (Oxford University Press, Oxford, 1993).
[11] S. Kralj and E. G. Virga, J. Phys. A **34**, 829 (2001).
[12] G. de Luca and A. D. Rey, J. Chem. Phys. **127**, 104902 (2007).
[13] W. H. Press, B. P. Flannery, S. A. Teukolsky, and W. Vetterling, *Numerical Recipies* (Cambridge University Press, Cambridge, 1986).
[14] N. Schopohl and T. J. Sluckin, J. Phys. (France) **49**, 1097 (1988).
[15] E. Penzenstadler and H. R. Trebin, J. Phys. (France) **50**, 1025 (1989).
[16] R. Rosso and E. G. Virga, J. Phys. A **29**, 4247 (1996).
[17] A. N. Pargellis, S. Green, and B. Yurke, Phys. Rev. E **49**, 4250 (1994).